Journal of Metals, Materials and Minerals, 36(4), e2563, 2026

Parring bamboo (*Gigantochloa atter*) composites as alternatives for safety cabin panels

Massriyady MASSAGUNI[1,*], Zulkifli DJAFAR[2,*], Rozli ZULKIFLI[3], and Lukmanul HAKIM ARMA[2]

[1] *ATI Makassar Polytechnic, Makassar, Indonesia*
[2] *Hasanuddin University, Department of Mechanical Engineering, Faculty of Engineering, Indonesia*
[3] *The National University of Malaysia, Department of Mechanical and Materials Engineering, Faculty of Engineering and Built Environment, Malaysia*

***Corresponding author e-mail**: massriyady.massaguni@atim.ac.id; zulkiflidjafar3065@gmail.com

Received date:
13 November 2025
Revised date:
7 April 2026
Accepted date:
8 June 2026

Keywords:
Composite;
Gigantochloa atter;
Safety cabin;
Mechanical properties;
Thermal properties

Abstract

This study aims to develop and evaluate a reinforced composite of Parring Bamboo (*Gigantochloa atter*) fiber with a Flame Retardant Polyester matrix (PaBFeR–FeReP). The study focuses on the effects of fiber treatment—comprising a combination of 5% NaOH alkalization and a water-based flame retardant inhibitor (FRI)—as well as fiber volume fraction variations (45%, 55%, and 65%) on material performance. The novelty of this research lies in mapping the synergy between layered fiber interface modification (chemical and flame retardant treatments) and a phosphorus-modified polyester matrix, a configuration that has not been comprehensively explored in Parring bamboo. Composite panels were fabricated using the hand-layup method and characterized via mechanical testing (tensile, flexural, impact), UL-94 burning test, TGA-DSC, SEM, and FTIR. The results showed that fiber treatment (NaOH and FRI) combined with a 65% fiber volume fraction (PFT65) provided the highest overall mechanical performance. Furthermore, all composite variants successfully achieved the UL-94 V-0 fire resistance classification without flaming droplets. Thermal analysis (TGA) indicated that the treatment advanced the initial decomposition temperature (T_{onset}), which accelerated the formation of a protective char layer (charring). Further DSC analysis confirmed the occurrence of charring or cross-linking processes at temperatures above 400°C, which supported thermal stability. The PaBFeR–FeReP composite shows promising initial potential as a more environmentally friendly alternative material. However, its suitability for application as safety cabin panels still requires further validation against specific engineering requirements and structural regulatory standards.

1. Introduction

In recent decades, the need for environmentally friendly, lightweight, and high-performance alternative metals has become increasingly urgent, especially for structural applications such as safety cabins. Natural fibre-based composites, including bamboo, have captured the world's attention due to their potential to reduce reliance on conventional materials while lowering carbon emissions. Gigantochloa atter, or parring bamboo, is one of the promising bamboo species due to its high mechanical strength, rapid growth, and abundant availability in tropical regions such as Indonesia, Malaysia, Thailand, and the Philippines. Among various bamboo species, Gigantochloa atter (Parring bamboo) is specifically selected for this study due to its uniquely thick culm walls and high fiber density, which inherently provide superior load-bearing capacity suitable for heavy structural applications compared to other local species.

Previous research has shown that natural fiber-based composites can achieve tensile and flexural strengths competitive with those of metals, especially when combined with a suitable polymer matrix. In addition, efforts to increase fire resistance in natural composite materials have been carried out through various methods, such as adding flame retardants and chemical treatments. However, despite its great potential, the use of Parring bamboo composite as a steel substitute for safety cabins still faces significant challenges, especially in terms of material consistency, resistance to dynamic loads, and performance in extreme conditions, such as fire and impact.

Some critical aspects of Parring bamboo composite as an alternative to steel remain unclear. First, the effects of fiber treatment variations and fiber composition on the mechanical properties of Parring bamboo composites have not been widely explored, even though these factors can significantly impact structural performance. Second, the effectiveness of various types of flame retardants in increasing the fire resistance of Parring bamboo composite has not been systematically compared, so there is no optimal formulation that can be adopted for safety cabin applications.

Previous research has provided an essential foundation in the development of Parring bamboo fiber composites. Previous studies by Massaguni *et al.* (2025) successfully enhanced the single-fiber strength and matrix compatibility of Parring bamboo through NaOH and flame-retardant (FR) treatments. However, a critical limitation remains: these treatments often create a trade-off where extended FR exposure degrades mechanical integrity. Furthermore, existing research has primarily focused on single-fiber behavior or generic polymer matrices, leaving a significant gap in understanding how layered interface modifications

behave collectively at the macroscopic panel level when paired with a phosphorus-modified flame-retardant polyester (FeReP) [1,2]

In the context of material applications, safety cabins are currently being developed to meet the increasing industrial need for special protection in high-temperature work environments and fire zones. The structure of the safety cabin panel typically consists of specialized material layers; it is fundamentally a laminated composite designed for both mechanical and thermal strength, usually made of alloy metal materials, such as Zinc Aluminum Alloy (Zn-xAl), and filled with Polyurethane with refractory substance treatment. The tensile strength of Zn-27Al reaches 441 MPa, the impact strength is 2.8 $kJ \cdot m^{-2}$, and the melting point reaches 488°C [3]. In addition, the latest findings on fire-retardant materials that lead to safety cabin applications, such as the findings of H Lavrenyuk *et al.* (2019) and B. Mychalichko *et al.* (2022), namely epoxy-amine composite materials modified with copper(II) hexafluorosilicate ($CuSiF_6$), FR materials specifically for wood have mechanical strength, tensile strength between 13.5 MPa and 17.2 MPa, and impact strength of 3.5 $kJ \cdot m^{-2}$ to 3.9 $kJ \cdot m^{-2}$ [4]. In TGA testing, this material has an onset temperature of 310°C to 322°C and a solid residue at 600°C of 20.7%. In the UL94 vertical burning test, this material has an after-flame time (AFT) of 11 s and an afterglow time (AGT) of 6 s, and meets the V1/middle standard for flame-retardant materials [4,5]. In addition, findings by E. Liu *et al.* (2025) on cellulose nanofibers/Polybenzoxazine-Polyvinyl alcohol (CNFs/PBZ-PVA), a super-light wood-based composite foam with a compressive strength of up to 2.57 MPa. TGA results show high thermal stability with significant carbon residues up to 600°C. UL-94 testing shows superior flame-retardant performance, with a V-0 classification, an after-flame time of less than 10 s, and an after-glow time of less than 5 s with no flaming droplets. The composite also exhibits hydrophobic properties [3]. These previous studies provide references on the achievement parameters for producing composite panels for safety cabin applications and comprehensively discuss two critical factors: mechanical and thermal properties.

This study aims to develop a bamboo-polymer composite with a Flame Retardant-Polyester (FR–P) matrix, also called PaBFeR–FeReP, as an alternative for safety-cabin applications that meet two main criteria: adequate mechanical strength and good fire resistance. The primary research gap addressed in this study is the inherent trade-off between fire resistance and mechanical strength in natural fiber composites, which remains inadequately solved for heavy structural applications. Consequently, the novelty of this research lies not merely in testing, but in mapping the synergy of a layered interfacial modification combining chemical alkalization and a water-based flame retardant inhibitor with a phosphorus-modified polyester matrix (FeReP) in Gigantochloa atter. This specific configuration aims to simultaneously satisfy the stringent mechanical and thermal stability requirements without compromising structural integrity. This material has not been widely explored for heavy structural applications. Some interesting topics to be discussed include the suitability of the PaBFeR–FeReP composite's strength for the safety cabin standard, both in terms of mechanical strength and thermal resistance.

This research contributes to multidimensional science. First, the results of this study will enrich the literature on the use of bamboo paring in structural composite materials, which remains very limited. Second, findings on fiber composition and compatible matrices serve as a reference for the development of nature-based refractory materials. Third, this research can be a pioneer in integrating green materials into safety cabin designs, opening up wider application opportunities in the construction, automotive, and defense industries. Thus, the study not only answers technical challenges but also contributes to global efforts to achieve sustainable development.

2. Method

2.1 Research stages

This research is carried out through several stages, systematically arranged to address the problem formulation and achieve the research objectives. The research stages span from the preparation of PaBFeR raw materials to the characterization of PaBFeR–FeReP composites, including mechanical, thermal, fire-resistance, and microstructural analysis. Each stage is designed to provide comprehensive information on the interaction between bamboo fiber paring and the FR–P matrix, so that a comprehensive picture of the potential of this material as an alternative to safety cabin panel material can be obtained. These stages are shown in the following Figure 1.

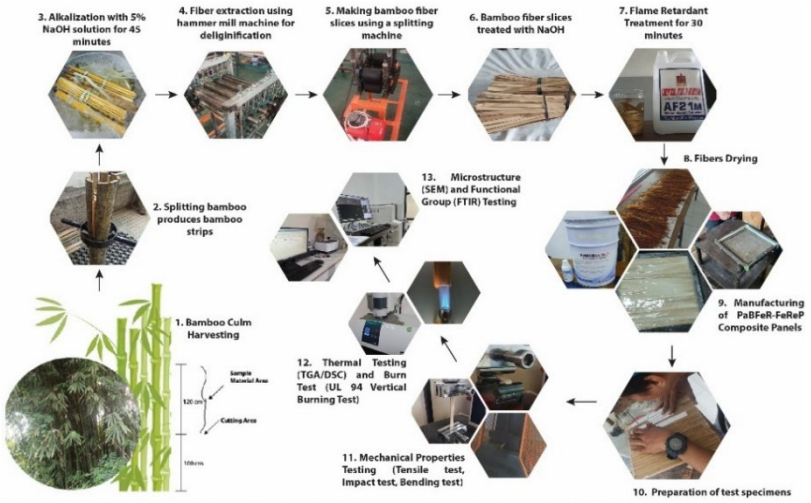

Figure 1. Stages of PaBFeR–FeReP research.

2.2 Materials

BaPFeR was collected from the Indonesian state of South Sulawesi, the city of Maros, and the village of Tanralili. The resin used is an Unsaturated Polyester Resin (UPR) type, Flame Retardant Polyester (FeReP), Merryhills Flame Retardant Polyester (FR–P) from Allensy Wooden, which is widely available on the market. This resin is a non-halogen thermoset with additives including Melamine Polyphosphate (MPP), Expendable Graphite (EG), and Boron compounds. The Delignification of PaBFeR uses Sodium Hydroxide (NaOH) solids sold over the counter. In addition, the Flame Retardant (FR) treatment on PaBFeR uses the water-based Flame Retardant Inhibitor (FRI) brand AKS Fire Inhibitor AF21Y, which is available in the market. This solution contains modified inorganic salts such as ammonium polyphosphate and ammonium sulfate.

2.3 Preparation of bamboo parring for PaBFeR–FeReP

PaBFeR is taken from a three-year-old Parring (PaB) bamboo stalk, with a cut point of 100 cm from the ground level, and then cut along 120 cm. Next, the PaB is split into strips using a special splitting knife. After splitting, the PaB strip is deignified by dissolving NaOH in water to 5% and soaking the strip for 45 min. After delignification, the PaB strips are processed in hammer mills for PaBFeR extraction and further processed on a splitting machine with a 5% NaOH treatment for 45 min, after which it is aerated at 30°Cfor 120 min. Untreated (normal) samples are also prepared at this stage without undergoing delignification or the hammer mill process. In contrast, the PaB strips are directly processed on the splitting machine, resulting in PaBFeR irradiation without NaOH treatment.

After obtaining two types of raw materials NaOH-treated PaBFeR and untreated PaBFeR NaOH-treated PaBFeR is soaked in FRI for 30 min, then aerated again at 30°C for 120 min. Meanwhile, PaBFeR without NaOH treatment was not immersed in FRI and prepared for normal condition PaBFeR–FeReP samples

2.4 PaBFeR–FeReP composite panel manufacturing

The PaBFeR–FeReP panel is made to measure 25 cm × 25 cm × 0.4 cm. The variation in fiber volume fractions of 45%, 55%, and 65% is calculated using the following equation [6]:

$$V_f = \frac{W_f/\rho_f}{W_f/\rho_f + W_m/\rho_m} \times 100\%$$

V_f = Volume fraction, W_f = Fiber weight, ρ_f = Density of fiber, W_m = Weight of matrix, and ρ_m = Matrix density. Density of BaPFeR = 0.76 g·cm^{-3} [7] whereas FeReP density = 1.129 g·cm^{-3} [8]. The fiber volume fractions of 45%, 55%, and 65% were strategically chosen based on typical structural composite optimization; fractions below 45% generally provide insufficient load transfer, whereas fractions exceeding 65% critically inhibit matrix impregnation, leading to severe void formations.

The variation of each composition of the PaBFeR–FeReP composite is shown in Table 1.

Table 1. Material composition of PaBFeR–FeReP.

Information	Variation		
	I	II	III
V_f PaBFeR [%]	45	55	65
V_f FeReP [%]	55	45	35
PaBFeR–FeReP volume [cm^3]	250	250	250
Vol PaBFeR [cm^3]	112.5	137.5	162.5
Vol FeReP [cm^3]	137.5	112.5	87.5
W_f PaBFeR [gr]	85.5	104.5	123.5
W_f FeReP [gr]	155.24	127.01	98.79
PaBFeR volume fraction [%]	45	55	65

The PaBFeR–FeReP panel is made by the hand-layup method, with a continuous/straight fiber orientation arranged on the mold, which has been given a wax release coating. After applying a wax release agent to the mold, the matrix and fibers were laminated and subsequently cured at room temperature (±27°C) with a relative humidity of ±65% for 24 h, followed by a post-curing process.

2.5 Sample preparation

In this study, samples were prepared based on treatment (normal) and no-treatment variation, and on fiber volume fraction variation. Sample codes are provided to make the data easier to search. Sample codes are designated as PF(N/T)XX%, where 'PF' stands for PaBFeR–FeReP. The code 'N' denotes 'Normal' (untreated fibers, lacking both NaOH and FRI treatments), while 'T' signifies fully 'Treated' fibers (subjected to both 5% NaOH alkalization and 30-min FRI soaking, XX% = Fiber volume fraction. Example: PFN45% = PaBFeR–FeReP without fiber treatment with a fiber volume fraction of 45%. The mechanical test samples prepared are tensile testing samples according to ASTM D638-14, impact testing according to ASTM D5942-96, and bending testing according to ASTM D790-17 [9–11]. The samples for microstructural analysis were obtained from the cross-sectional fractured surfaces of the specimens following the tensile tests, cut to an approximate size of 5 mm × 5 mm × 4 mm. The sample for functional group analysis was prepared according to the Fourier transform infrared spectroscopy (FTIR) sample protocol, in the form of a powder, from the PaBFeR–FeReP panel that had been made. In addition, the Simultaneous Thermal Analysis (STA) thermal test was prepared, test samples were prepared according to the Thermogravimetric analysis (TGA) and Differential scanning calorimetry (DSC) tests measuring 5 mm × 4 mm × 4 mm and the combustion test was prepared samples according to the vertical burning test of Underwriters Laboratories 94 (UL94), the samples tested were in the form of a rod with a standard size of 125 mm × 13 mm and a thickness according to the thickness of the panel of 4 mm. Mechanical testing and composite combustion testing are prepared 7 samples each for each variation.

2.6 Mechanical testing

Tensile and bending tests of the PaBFeR–FeReP composite were performed using an LR10K universal testing machine with a 10 kN load cell from Ametek. Tensile testing is performed at a tensile speed of 1 mm·min^{-1}, while bending testing is performed at a compressive

speed of 1 mm·min^{-1}. Impact testing using Zwick Roell brand machines with a capacity of 5 J to 50 J, with a pendulum mass of 5.78 kg, and an arm length of 0.42 m.

2.7 Microstructure analysis

SEM testing using the JED-2300 Analysis Station Plus brand JEOL's DrySDTM. Composites are observed at 1000x magnification, with a bar scale of 20 μm. The focus of the analysis is on voids and gaps that occur during fabrication or as a result of treatment applied to the composite.

2.8 Analysis of function clusters

Analysis of the functional group using the QATRTM brand FTIR test tool from Shimadzu Corporation. The observed wavelengths range from 500 cm^{-1} to 4000 cm^{-1} with a resolution of 2 cm^{-1}. The focus of the observation was on the functional groups formed as a function of fiber volume fraction and flame retardants.

2.9 Burning test

The burning test is conducted in accordance with the UL 94 vertical burning test standard to determine the classification of PaBFeR–FeReP fire resistance under flame exposure. The test equipment consists of a tirrill burner supplied with fuel gas based on propane (C_3H_8) and butane (C_4H_{10}) gas, namely Liquefied petroleum gas (LPG), a control valve, a flowmeter, a manometer, a clamp, cotton as an indicator of light droplets, and a combustion cabin with an observation window. The test sample is a composite panel positioned vertically on the clamp. The test procedure is carried out by lighting the burner and directing the flame to the bottom of the sample for 10 s, then recording the after-flame time until the flame is extinguished. The flame was then redirected to the exact location for 10 s, and a second later, the afterflame was recorded. After the flame goes out, the afterglow time is recorded until the sample no longer shows flame or flame. During the test, flammable material droplets and the potential for cotton ignition under the sample were observed. The classification of results is differentiated into V-0, V-1, and V-2. Category V-0 is given when each specimen has a flame time of no more than 10 s, the total afterflame of the entire specimen is not more than 50 s, no flaming droplets are igniting the cotton, and the flame does not reach the clamp. The V-1 classification has similar requirements but allows a power time of up to 30 s with a maximum total of 250 s. Meanwhile, the V-2 is the same as the V-1 but enables the droplets to ignite as long as the cotton underneath does not burn.

2.10 Thermal analysis

STA with TGA-DSC uses the STA 449 Jupiter brand test equipment from Netzsch. The setup parameters are 25°C to 600°C using N_2 gas, with a gas flow of 50 mL·min^{-1} and a heating rate of 10°C·min^{-1}. Chart standards based on the International Confederation of Thermal analysis and calorimetry (ICTAC). In this test, the melting heat and Charring/cross-linking heat can be calculated using the formula:

$$\Delta H = \frac{\text{Area under the melting or charring peak}}{\text{Cooling or heating rate}}$$

ΔH = Heat of Charring/cross-linking/melting (J·g^{-1}), area under the melting or Charring/cross-linking peak (W·°C^{-1}·g^{-1}) (obtained directly from Netzsch graph analysis software), and cooling or heating rate (°C·s^{-1}) obtained from the research set-up (10°C·min^{-1} = 0.17 °C·s^{-1}). Furthermore, baseline correction (baseline subtraction) was properly applied to all DSC curves using the Netzsch analysis software prior to the quantitative extraction of the enthalpy (ΔH) areas to ensure accurate reading.

2.11 Data analysis

The mechanical test results were statistically analyzed using the Variance Analysis (ANOVA) method to determine the significant influence of fiber treatment (normal vs. treatment) and fiber volume fractions (45%, 55%, and 65%) on the mechanical properties of the composites. One-way ANOVA is used for each test parameter, with $\alpha = 0.05$. Prior to ANOVA, the assumptions of data normality and variance homogeneity were verified using the Shapiro-Wilk and Levene's tests, respectively. If ANOVA shows significant differences between groups, a follow-up test, such as Tukey's Honestly significant difference (HSD), is used to determine which group pairs differ significantly. The results of microstructural testing using SEM were qualitatively analyzed by visual inspection of surface morphology, fiber distribution, voids, and matrix-fiber interactions. Functional group analysis by FTIR was used to identify changes in chemical bonds resulting from NaOH and FRI treatments, as well as the involvement of active functional groups in the composites. UL-94 vertical combustion test data is analyzed based on afterflame time, afterglow, presence of ignited droplets, and V-0, V-1, and V-2 standard classifications. Combustion visualization using a macro camera. Thermal analysis using TGA-DSC was performed to determine the initial degradation temperature (T_{onset}), the maximum degradation temperature (T_{max}), the residue, and the heat flow values related to the thermal stability and Charring/cross-linking properties of the composites. The results are presented in tables and graphs, and then interpreted to explain the relationships among fiber treatment, volume fraction, mechanical properties, fire resistance, and thermal stability of PaBFeR–FeReP composites.

3. Result and discussion

3.1 Mechanical properties

The results of the mechanical test of PaBFeR–FeReP are shown in Table 2. Table 2 summarizes the mechanical properties of PaBFeR–FeReP composites under two fiber conditions, namely PFN (untreated) and PFT (with treatment), respectively, at fiber volume fractions of 45%, 55%, and 65%. The parameters presented include tensile, bending, and impact strengths. All values are reported as the average ± standard deviation for each sample code.

Based on Table 2, there is a consistent upward trend in mechanical strength (tensile, flexural, and impact) as the fiber volume fraction increases from 45% to 65%. Furthermore, the application of interfacial fiber treatment effectively enhances the load-transfer capacity of the material, with the treated sample group (PFT) consistently outperforming the untreated samples (PFN) across all composition levels. Peak mechanical performance is achieved by the PFT65% variant, which

records the highest tensile strength of 57.41 MPa, flexural strength of 112.84 MPa, and impact toughness of 46.89 kJ·m^{-2}. From an engineering perspective, the dominance of these values in PFT65%, combined with a lower strain (1.06% in the tensile test), indicates that the synergy between a dense fiber volume and chemical modification produces a material that is not only stiff but also tough in absorbing shock energy. This mechanical toughness profile makes the PaBFeR–FeReP composite highly relevant and promising for withstanding moderate dynamic loads in structural applications such as safety cabin panels.

A visualization series of PaBFeR–FeReP composite tensile test results on the entire sample code (PFN/PFT; 45% to 65% V_f), covering a summary of the average value, statistical test output, tensile strength–tensile strain curve, and tensile tensile relationship, is shown in Figure 2 below.

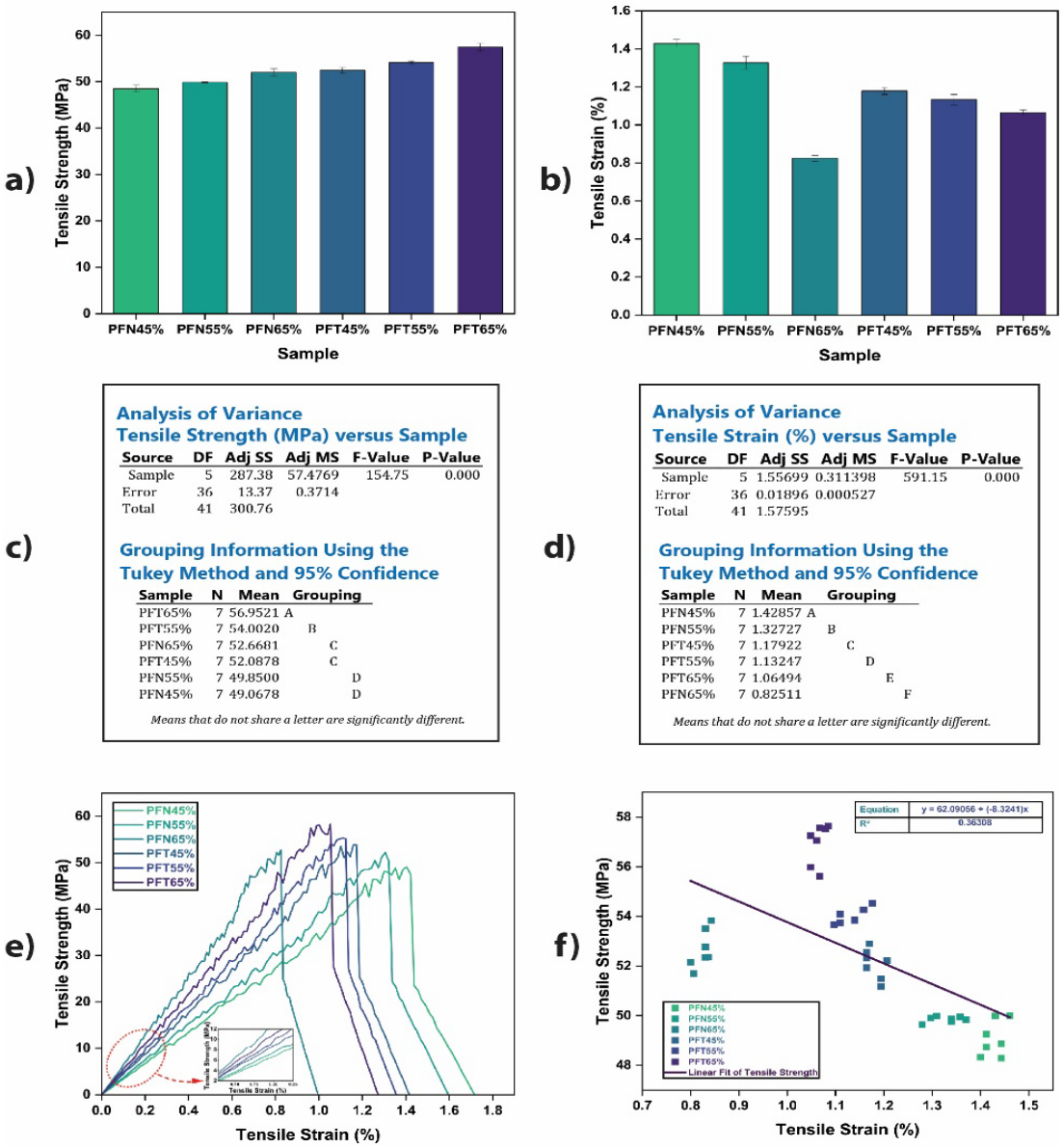

Figure 2. (a) Tensile strength, (b) Tensile strain, (c) ANOVA & Tukey output—tensile strength, (d) ANOVA & Tukey output—tensile strain, (e) Tensile strength–strain curve, and (f) tensile strength vs tensile strain relationship.

Table 2. PaBFeR–FeReP mechanical test results.

No.	Sample code	Tensile strength [MPa]	Tensile strain [%]	Bending strength [MPa]	Bending strain [%]	Impact strength [kJ·m^{-2}]
1	PFN45%	48.51 ± 0.71	1.43 ± 0.02	92.92 ± 2.52	1.37 ± 0.07	30.21 ± 2.50
2	PFN55%	49.88 ± 0.12	1.33 ± 0.03	104.68 ± 2.01	1.45 ± 0.03	39.91 ± 1.83
3	PFN65%	52.03 ± 0.76	0.83 ± 0.02	110.74 ± 2.28	1.58 ± 0.18	43.60 ± 0.39
4	PFT45%	52.42 ± 0.60	1.18 ± 0.02	93.78 ± 2.40	1.31 ± 0.01	35.74 ± 0.14
5	PFT55%	54.10 ± 0.31	1.13 ± 0.03	105.02 ± 1.90	1.36 ± 0.02	42.21 ± 0.08
6	PFT65%	57.41 ± 0.82	1.06 ± 0.01	112.84 ± 2.13	1.45 ± 0.11	46.89 ± 0.13

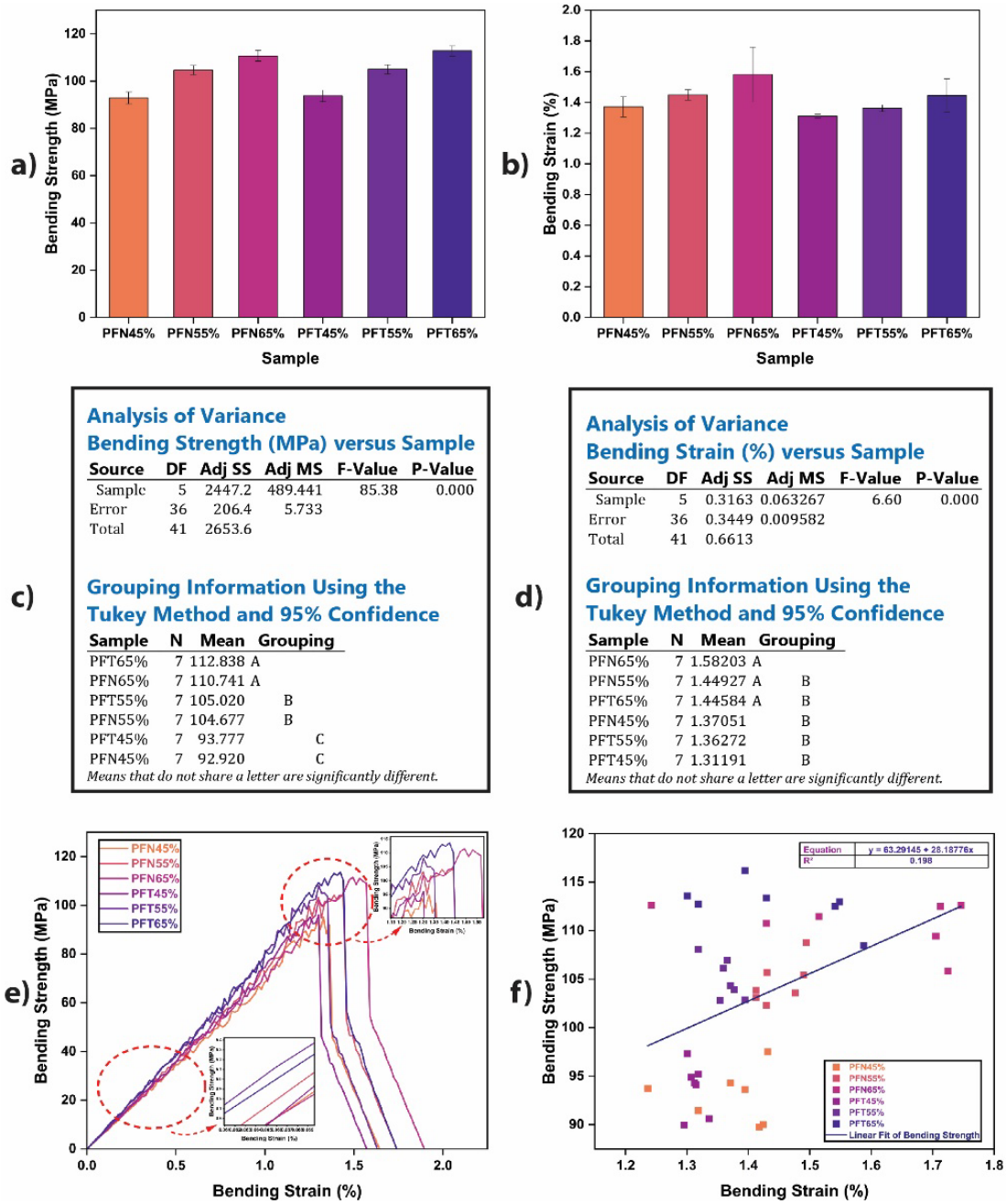

Figure 3. (a) Bending strength, (b) bending strain, (c) output ANOVA & Tukey—bending strength, (d) ANOVA & Tukey output—bending strain, (e) bending strength–bending strain curve, and (f) strength vs strain bending relationship.

A comprehensive analysis of Figure 2 demonstrates a clear correlation between tensile strength and strain; as the fiber volume fraction increases, the tensile strength significantly improves while the elongation at break decreases. Linear regression analysis and statistical grouping (ANOVA/Tukey) confirm that the application of layered interfacial modifications (NaOH and FRI) in the treated group (PFT) effectively restricts the deformation of the polyester matrix, shifting the composite profile to become stiffer yet possessing a substantially higher tensile load-bearing capacity. When compared to findings in the literature, the mechanical performance achieved by the PaBFeR–FeReP composite outperforms short and randomly oriented bamboo-epoxy composites, which typically plateau at a strength of around 32 MPa [12]. Mechanistically, this enhancement in tensile stress is driven not only by the unidirectional continuous fiber architecture but also by the synergistic effects of interfacial modification. The NaOH alkalization process successfully removes residual lignin to create strong mechanical interlocking [13,14], while the phosphorus-based compounds from the flame retardant inhibitor (FRI) potentially facilitate the formation of additional secondary bonds with the polyester matrix. This mechanochemical synergy facilitates a highly efficient stress transfer from the matrix to the reinforcing fibers, effectively resisting crack propagation and preventing premature fiber pull-out phenomena compared to the untreated composite systems.

A series of visualizations of PaBFeR–FeReP composite bending test results on all sample codes (PFN/PFT; 45% to 65% V_f) includes a summary of the average value, statistical test output, bending strength–

bending strain curve, and bending strength-bending strain relationship shown in Figure 3. Referring to Figure 3, the flexural (bending) behavior profile of the composite exhibits a strengthening trend consistent with the tensile test; an increase in the fiber volume fraction accompanied by layered interfacial modification (PFT) significantly boosts the composite's capacity to withstand bending deformation. Mechanistically, this increase in flexural stress confirms that the synergy of lignin removal via NaOH alkalization and the addition of the phosphorus-based Flame retardant inhibitor (FRI) effectively improves the quality of interfacial adhesion. This, in turn, successfully mitigates potential interlaminar shear failure when the material is subjected to transverse loads. When compared with previous literature, the flexural performance of PaBFeR–FeReP outperforms short, randomly oriented bamboo-epoxy composites as well as systems relying solely on conventional alkali/silane modifications, which typically plateau at strengths around 70 MPa to 87 MPa [15]. The mechanical superiority in our study is fundamentally contributed by the use of a unidirectional continuous fiber architecture, which distributes bending stress much more efficiently than random fiber schemes. Although the achieved flexural values cannot yet match laminated composites with aggressive Graphene oxide (GO) treatments that can exceed 260 MPa [16], the structural stiffness profile generated by the PaBFeR–FeReP composite is considered highly competitive. This performance affirms that the material possesses adequate resistance to dynamic bending loads, a crucial engineering qualification required for structural safety cabin panel applications.

A series of visualizations of the results of the PaBFeR–FeReP composite impact test results on the entire sample code (PFN/PFT; 45% to 65% V_f), including a summary of the average values and statistical test outputs of ANOVA and Tukey HS, are shown in the following Figure 4.

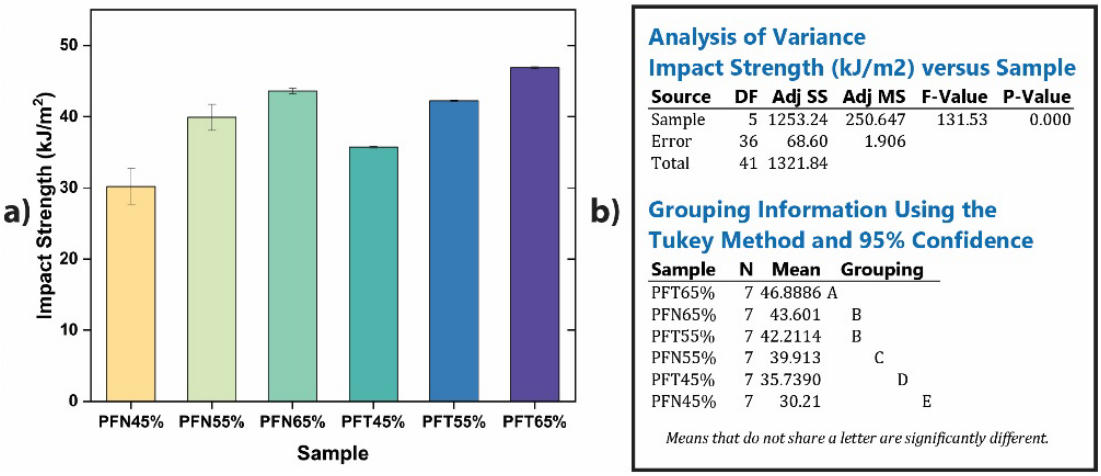

Figure 4. (a) Impact strength, and (b) ANOVA & Tukey output—impact strength.

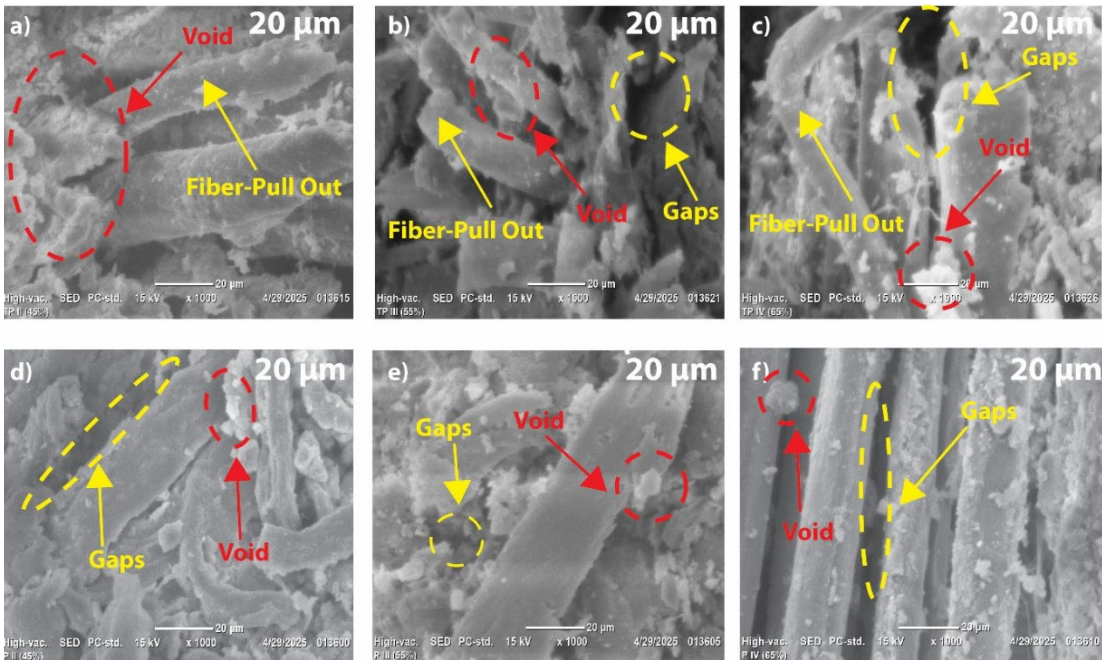

Figure 5. SEM micrographs of fractured surfaces post-tensile testing showing the failure mechanisms and matrix-fiber interfaces of: (a) PFN45% exhibiting severe fiber pull-out and large voids, (b) PFN55%, (c) PFN65%, (d) PFT45%, (e) PFT55%, and (f) PFT65% demonstrating dense matrix impregnation, minimized interfacial gaps, and dominant fiber breakage mechanisms.

In Figure 4, the PaBFeR–FeReP composite exhibits a consistent upward trend with increasing fiber volume fraction and the application of interfacial modification (PFT). Mechanistically, the achievement of the highest energy toughness in the PFT65% variant indicates that the layered treatment (NaOH alkalization and FRI phosphorus agent) successfully optimizes the matrix-fiber interfacial bond without compromising intrastructural flexibility; this allows the material to effectively absorb and dissipate impact energy through fiber bridging mechanisms and the arrest of crack propagation. When compared with previous literature, the impact performance of PaBFeR–FeReP significantly outperforms conventional short-fiber bamboo-epoxy composites as well as untreated systems fabricated via VARTM, which are generally only capable of absorbing energy at levels of 5.4 kJ·m^{-2} [17] to 8.4 kJ·m^{-2} [18]. This extreme superiority is fundamentally driven by the employment of a unidirectional continuous fiber architecture, which resists shock load propagation far more efficiently than random fiber configurations. Furthermore, this toughness achievement proves highly competitive even when juxtaposed with bamboo composites specifically optimized using Response surface methodology (RSM), which plateau around 39.3 kJ·m^{-2} [19]. This superior energy absorption performance directly validates the viability of the PaBFeR–FeReP composite in dampening sudden dynamic impacts, an absolute prerequisite for safety cabin panel materials.

3.2 Microstructure

The SEM results are shown in Figure 5. SEM observations were conducted on the fractured surfaces of post-tensile specimens to comprehensively evaluate the failure mechanisms. Based on Figure 5, a significant transition in failure mechanisms is evident between the sample groups. In the untreated series (PFN), the interfacial topography appears open, featuring deep fiber pull-out tracks and large matrix voids. Semi-quantitatively, the interfacial gaps in the PFN samples are relatively wide due to the poor compatibility between the hydrophilic fibers and the hydrophobic polyester. Conversely, in the layered treatment series (PFT), the matrix tightly envelops the fiber contours. Specifically, in PFT65% (Figure 5(f)), the fiber bundle structure is highly compact, and interfacial gaps are significantly reduced. The failure mechanism in PFT65% is no longer dominated by fiber pull-out but rather by fiber breakage and matrix micro-cracking. Mechanistically, this confirms that the removal of lignin via alkalization and the binding effect of the phosphorus FRI agent facilitated superior mechanical interlocking, allowing the tensile stress to be optimally transferred up to the fiber's intrinsic ultimate strength before failure occurred.

The pattern is in line with recent research that alkaline treatment of bamboo fibers improves the bonding of the interface and improves the mechanical properties of composites. NaOH treatment research with SEM evidence in the form of a cleaner and rougher fiber surface, so that adhesion increases [20]. Other research has shown that the lumen and tissue of the resin parenchyma of bamboo trigger the pull of fibers and cavities on the fracture, thus limiting strength; Improvement recommendations are directed at surface modification and reduction of bundle diameter for better resin penetration, consistent with our observations at high fractions [21]. In addition, the results of other studies confirm that porosity and void decrease the tensile strength and toughness of composites because they interfere with the load transfer pathway and trigger the initiation of cracks; This trend applies across fiber systems, including natural fiber composites [22,23]. The combination of evidence reinforces the interpretation that gap reduction and interface adhesion improvement—as seen in the treatment series—are key to improving the mechanical performance of PaBFeR–FeReP panels.

3.3 Function group

The results of the function group using FTIR are shown in Figure 6 To provide deeper chemical insight into the composite's superior performance, the FTIR spectra confirm a specific interactive synergy at the fiber-matrix interface. The removal of lignin via NaOH alkalization exposes a higher density of reactive cellulosic hydroxyl (O–H) sites. These exposed sites act as chemical anchors for the phosphate compounds (P–O–C) from the FRI agent, facilitating the formation of extensive secondary hydrogen bonds without degrading the integrity of the matrix's carbonyl (C=O) backbone. This specific interfacial bonding mechanism—rather than the mere physical presence of phosphate—fundamentally explains why the highly treated samples (e.g., PFT65%) can withstand significantly higher mechanical stress and arrest crack propagation. Furthermore, this tight mechanochemical interlocking prevents premature devolatilization, allowing the phosphorus species to efficiently catalyze a denser protective char layer during thermal degradation, advancing beyond the standard flame-retardancy mechanisms of conventional polyesters [24,25].

3.4 Burn resistance

The results of the combustion test with the UL94 vertical combustion test standard are shown in the following Table 3.

The results of the vertical combustion test showed that all composite variants met the UL-94 V-0 classification: no flame droplets, no cotton burns, and the flame did not reach the clamp. The afterflame time was recorded at zero in most samples; only PFN65% (t_1 = 0,71 s) and PFT45% (t_1 = 0,57 s) showed momentary flame, with t_2 = 0 s and t_3 = 0 s in all samples. With a flame time per specimen of less than 10 s and a total of less than 50 s, the V-0 criteria are met as per the UL-94 procedure used.

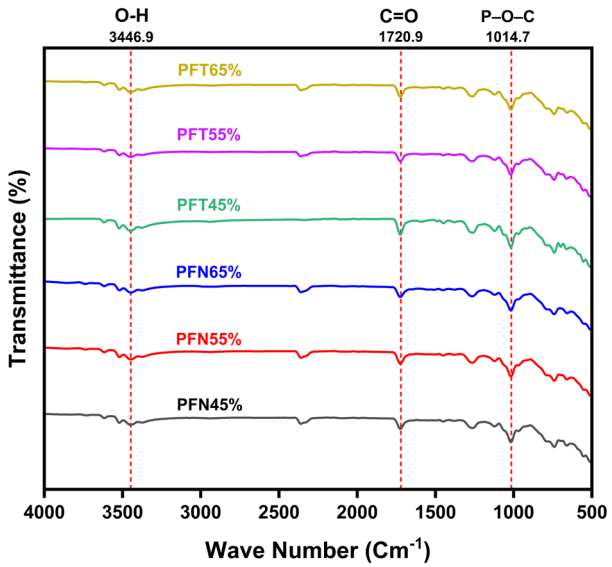

Figure 6. Graphic FTIR PaBFeR–FeReP.

Table 3. PaBFeR–FeReP burn test results.

No.	Sample code	After flame time, t_1 [s]	After flame time, t_2 [s]	After glow time, t_3 [s]	Flame drops	Cotton burns	Burnt to clamp	UL 94 classification
1	PFN45%	0	0	0	No	No	No	V_0
2	PFN55%	0	0	0	No	No	No	V_0
3	PFN65%	0,71	0	0	No	No	No	V_0
4	PFT45%	0,57	0	0	No	No	No	V_0
5	PFT55%	0	0	0	No	No	No	V_0
6	PFT65%	0	0	0	No	No	No	V_0

Table 4. TGA PaBFeR–FeReP test results.

No	Kode sampel	Heating rate [°C·s^{-1}]	T_{onset} [°C]	T_{maks} [°C]	T_{finish} [°C]	Residu [%]	LOI [%]
1	PFN45%	0.17	248.54	342.02	454.11	37.03	61.74
2	PFN55%	0.17	250.01	340.90	437.66	39.33	60.58
3	PFN65%	0.17	224.60	340.59	459.93	37.73	62.01
4	PFT45%	0.17	228.59	337.91	460.63	32.12	67.82
5	PFT55%	0,17	218,55	335,74	453,69	37,56	62,01
6	PFT65%	0,17	214,93	333,12	445,10	37,46	62,28

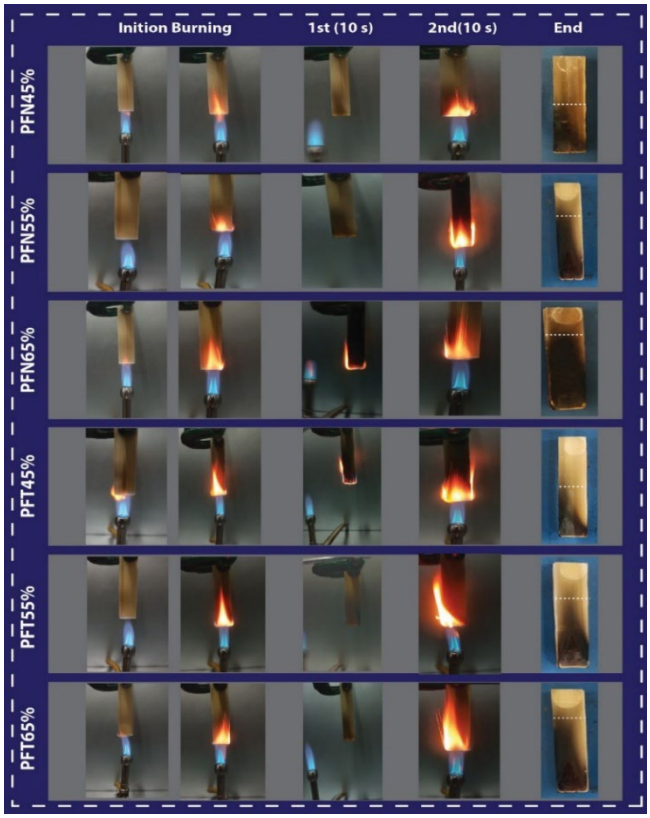

Figure 7. BaPFeR-FeReP burning test visualization.

The burn test is shown in the following Figure 7. The vertical test visualization shows the burning response of each sample in the initial ignition phase, the first 10 s of exposure, the second 10 s of exposure, and the final condition. All specimens show self-extinguishing as soon as the fire source is moved, with no flame droplets or flammable clamps. The charcoal zone forms only on the lower segment of the specimen, and the charcoal height is relatively short, with momentary traces of flame only visible in a small portion of the image. This visual pattern is consistent with the results of the table; all variants meet the V-0 criteria, and only PFN65% and PFT45% showed a very short flame on the first exposure.

The behavior of V-0 in flame-retardant polyester matrices and natural fiber composites is generally attributed to a phosphorus-based solid-phase mechanism that forms a protective charcoal layer and inhibits heat diffusion and flammable volatiles. The results of recent research on unsaturated polyester confirm that an adequate phosphorus-based strategy is able to achieve V-0 in the UL-94 test. In addition, natural fiber composite studies show that phosphorus-based formulations, or synergies with expansive additives such as expandable graphite or MPP/APP, are effective in reducing flame propagation and extinguishing time, in line with visual observations of high charcoal layers and the absence of ignited droplets in specimens. The finding that V-0 in UPR is commonly achieved when the effective phosphorus content exceeds a certain threshold is also in line with recent research on modified UPR systems. At the same time, another study on bamboo composites showed that phosphorus-based activation increased the UL-94 rating towards V-0. These patterns support the interpretation that the combination of the FR–P matrix and the fiber treatment on these panels results in an efficient charcoal formation pathway so that the specimen extinguishes on its own and meets the highest classification of UL-94 [26–28].

3.5 Thermal properties

The results of the TGA test using STA (DSC/TG) are shown in the following Table 4.

At a heating rate of 0.17°C·s^{-1}, the thermal parameters are in the following range: Tonset 214.93°C to 250.01°C, with a tendency of PFN values higher than PFT; Tmax 333.12°C to 342.02°C, again higher in the PFN series; and Tfinish 437.66°C to 460.63°C, highest at PFT45% and PFN65% and lowest at PFN55%. Final residues range from 32.12% to 39.33%, with a maximum at PFN55% and a minimum at PFT45%. The LOI value was at 60.58% to 67.82%, highest in the PFT45% and relatively uniform (60% to 62%) in the other samples. The rate of temperature decrease in the mass of the sample is shown in the following Figure 8.

Figure 8(a–c) present the thermogravimetric analysis (TGA), mass loss profiles, and derivative thermogravimetry (DTG) curves for all PaBFeR–FeReP samples. The thermal degradation generally occurs in three main stages: initial moisture release (<100°C), primary pyrolysis at the Tonset region (214°C to 250°C), and final decomposition concluding around 450 °C. The treated samples (PFTs) consistently exhibit an earlier Tonset and a broader DTG peak (Figure 8(c)) compared to the untreated group (PFNs). Specifically, the maximum mass loss rate temperature (T_{max}) shifted from 341°C in the PFNs down to 333.1°C in PFT65%. This earlier degradation onset confirms the solid-phase flame-retardant mechanism, where the phosphorus agent catalyzes rapid dehydration to build a protective char layer. Consequently, the final residue (Figure 8(b)) is maintained at a high level (up to 37.46% for PFT65%), demonstrating that the composite degrades in a significantly more controlled manner.

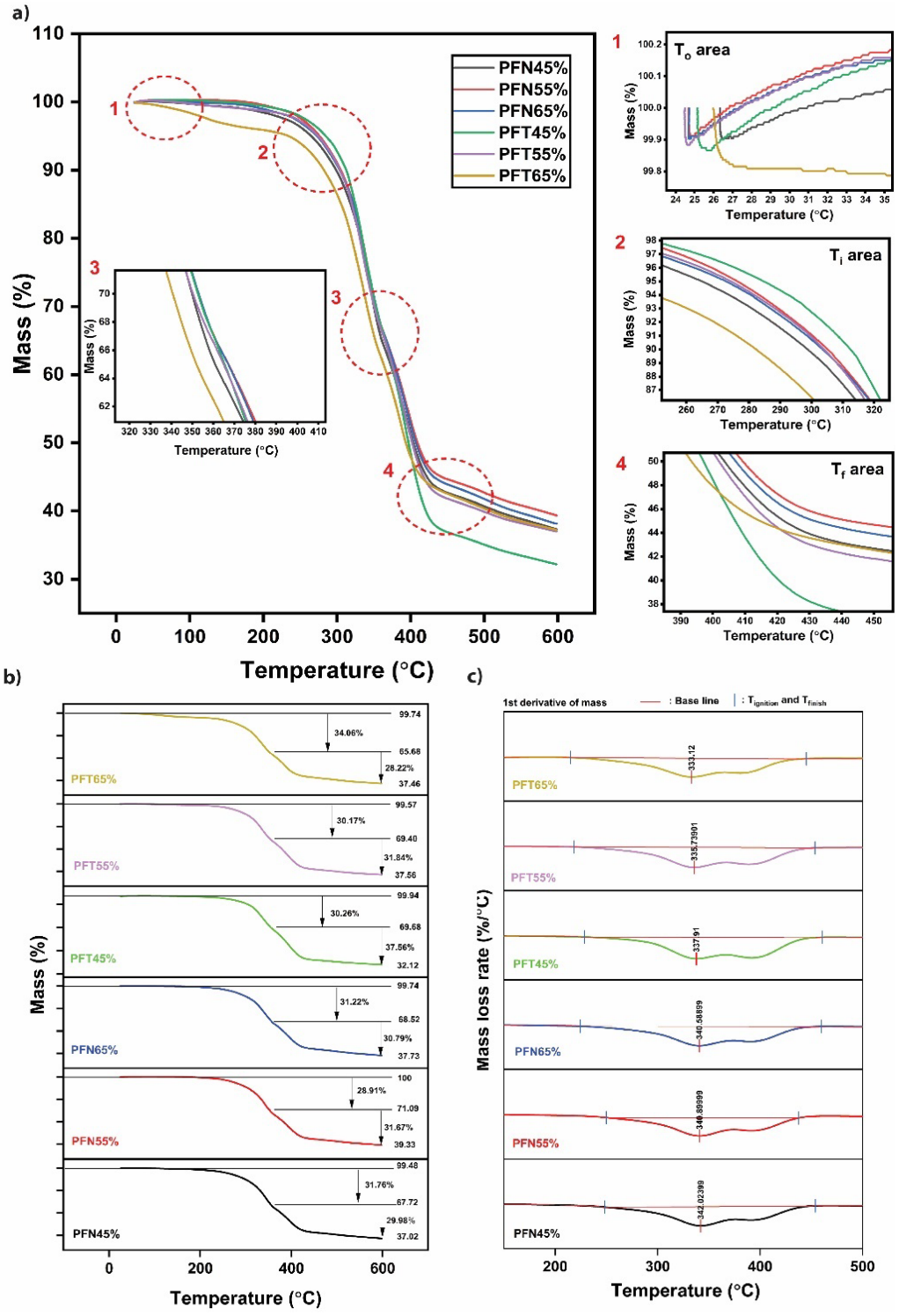

Figure 8. (a) TGA BaPFeR-FeReP graph and segmentation of each zone, (b) mass loss and residue profiles per sample, and (c) DTG curve and T_{onset} and T_{finish} characterization, along with peak mass loss rate.

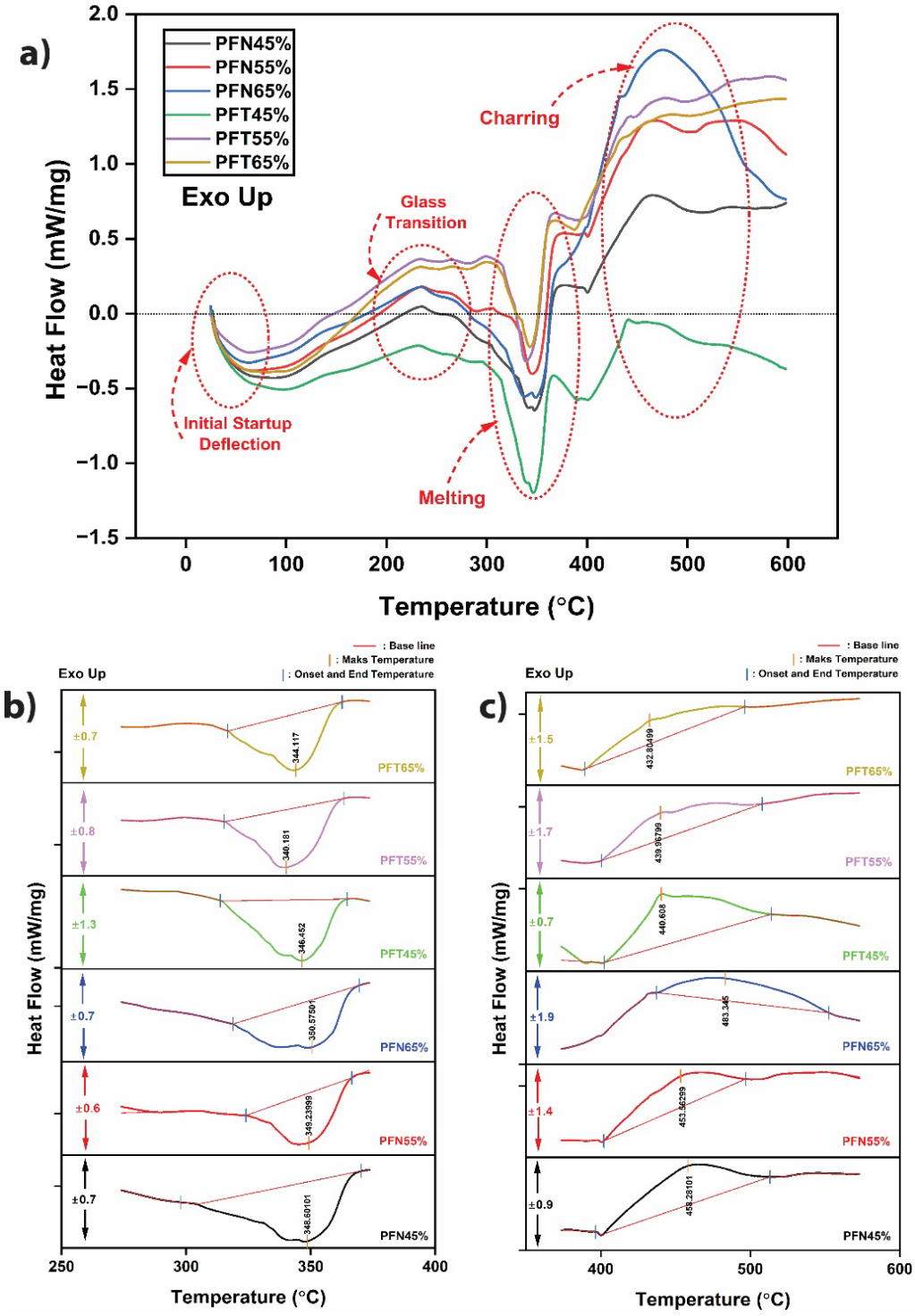

Figure 9. (a) DSC BaPFeR-FeReP Curve (Exo up), (b) DSC BaPFeR-FeReP melting area curve, and (c) DSC BaPFeR-FeReP Charring/cross-linking area curve.

Table 5. DSC test results for endothermic/ melting data.

No.	Sample	T_{onset} [°C]	T_{maks} [°C]	T_{end} [°C]	Area under the melting peak [W·°C^{-1}·g^{-1}]	Heating rate [°C·s^{-1}]	ΔH_m [J·g^{-1}]
1	PFN45%	297.8	348.6	370.32	23.38	0.17	140.268
2	PFN55%	324.03	349.24	366.54	15.47	0.17	92.80
3	PFN65%	318.86	350.58	369.47	19.41	0.17	116.46
4	PFT45%	313.76	346.45	350.58	21.71	0.17	130.25
5	PFT55%	315.37	340.18	363.39	21.40	0.17	128.43
6	PFT65%	316.784	344.117	362.64001	16.56	0.17	99.35

Table 6. DSC test results for exothermic/charring/cross-linking data.

No.	Sample	T_{onset} [°C]	T_{maks} [°C]	T_{end} [°C]	Area under the charring/cross-linking peak [W·°C^{-1}·g^{-1}]	Cooling rate [°C·s^{-1}]	ΔH_c [J·g^{-1}]
1	PFN45%	396.53	458.28	513.17	22.60	0.17	135.60
2	PFN55%	402.03	453.56	496.93	19.90	0.17	119.39
3	PFN65%	399.63	473.06	566.37	105.99	0.17	635.93
4	PFT45%	402.34	440.61	514.07	22.57	0.17	135.40
5	PFT55%	400.45	439.97	508.03	22.86	0.17	137.17
6	PFT65%	389.43	432.80	496.31	17.61	0.17	105.65

The results of DSC analysis using STA (DSC/TG) are shown in Table 5 for endothermic/melting data, and Table 6 for the following exothermic/charring/cross-linking data.

As detailed in Table 5-6, the DSC parameters reveal a distinct shift in the thermal transition of the treated composites. The PFT series generally exhibits slightly lower peak melting temperatures and a more uniform melting window compared to the untreated (PFN) group. More importantly, during the exothermic phase (>400°C), the treated samples demonstrate an earlier onset of charring and cross-linking with a more moderated heat release (ΔHchar). This accelerated but highly controlled thermal response confirms that the layered interface treatment successfully promotes early protective char formation, rather than allowing a sudden and catastrophic thermal degradation. The DSC graph is shown in the following Figure 9.

Thermally, the treated samples (e.g., PFT65%) exhibit an earlier Tonset (214.93°C) compared to the untreated PFN65% (224.60°C). Rather than indicating thermal weakness, this early onset, followed by a broader and more controlled mass loss rate (DTG peak), demonstrates the successful condensed-phase mechanism of the FRI agent. The phosphorus compounds catalyze rapid dehydration to form a dense protective char layer. Furthermore, DSC analysis clarifies the distinct thermal events: the endothermic peak (~344°C) corresponds to the melting of the polyester matrix, while the massive exothermic peak (>400°C) represents robust char formation and cross-linking, not crystallization. Ultimately, the PFT65% composite is deemed optimal not merely based on relative statistical trends, but because its specific thermal mechanism—sacrificing early decomposition to build a highly stable char barrier (maintaining a 37.46% solid residue)—directly meets the stringent engineering requirement for safety cabin panels to resist heat diffusion and prevent catastrophic structural collapse during a fire event.

4. Conclusion

Based on the results of the study on Parring Bamboo fiber-reinforced flame-retardant polyester (PaBFeR–FeReP) composites for safety cabin panel applications. Through systematic variations in fiber volume fraction and layered interfacial treatments (NaOH and FRI), the composite demonstrating the best performance balance was achieved at a 65% treated fiber volume fraction (PFT65%). The selection of this variant is not merely based on peak statistical values, but specifically on its ability to meet stringent safety engineering requirements. Mechanically, PFT65% achieved peak tensile (57.41 MPa), flexural (112.84 MPa), and impact toughness (46.89 kJ·m^{-2}), demonstrating the necessary stiffness and capacity to absorb dynamic shock loads crucial for cabin structural integrity. Thermally, the composite successfully achieved a UL-94 V-0 classification, indicating rapid self-extinguishing capabilities without flaming droplets. Furthermore, TGA and DSC evaluations confirmed that the treatment facilitated an earlier initial degradation (Tonset 214.93°C) followed by robust protective char formation (>400°C exothermic phase, maintaining a 37.46% solid residue). This thermal mechanism acts as an essential barrier to prevent heat diffusion and fire propagation. Ultimately, the mechanochemical synergy of the continuous fiber architecture and layered modification validates the PFT65% composite as a highly viable alternative material for heavy-duty safety cabin panel structures.

CRediT authorship contribution statement

M. Massaguni: Writing – review & editing, Writing – original draft, Visualisation, Project administration, Methodology, Investigation, Conceptualisation.

Z. Djafar: Supervision, Visualisation, Validation, Methodology, Investigation, Formal analysis, Data curation, Conceptualisation.

R. Zulkifli: Supervision, Validation, Formal analysis, Data curation.

L.H. Arma: Supervision, Investigation, Conceptualisation.

Declaration of competing interest

The authors declare that they have no known competing financial interests or personal relationships that could have appeared to influence the work reported in this paper.

Data availability

Data will be made available on request.

Acknowledgements

Thank you to the composite research team at the Applied Mechanics Laboratory, Department of Mechanical Engineering, Faculty of Engineering, Hasanuddin University, who have contributed to the smooth running of this research. In addition, we thank the Kementerian Pendidikan Tinggi, Sains, dan Teknologi, which has provided funding for the Hiliriset 2026 dan 2027 programs.

Reference

[1] M. Massaguni, Z. Djafar, R. Zulkifli, and L. Hakim "Enhancing mechanical strength of bamboo parring (*Gigantochloa atter*)

fiber with alkaline treatment for flame - retardant composite," *Discover Materials*, vol. 5, p. 136, 2025.

[2] M. Massaguni, Z. Djafar, R. Zulkifli, and L. H. Arma, "Adhesion strength of parring bamboo (*Gigantochloa atter*) fiber with flame retardant polyester resin : Wettability," *Material Design & Processing Communications*, vol. 2015, no. 1, 2025.

[3] E. Liu, M. Chen, Y. Chang, H. Zhang, and Z. Wu, "Sustainable super-light and high-strength wood-based composite foam with hydrophobic, flame-retardant and thermal-insulating properties," *Industrial Crops and Products*, vol. 233, p. 121500, 2025.

[4] H. Lavrenyuk, V. P. Parhomenko, and B. Mykhalichko, "The effect of preparation technology and the complexing on the service properties of self-extinguishing copper(II) coordinated epoxy-amine composites for pouring polymer floors. *International Journal of Technology*, vol. 10, pp. 290–299, 2019.

[5] B. Mykhalichko, and H. Lavrenyuk, "Flame protection technologies for wood: Developing and testing for fire of timbers with a flame-retardant coating based on the epoxy-amine composite modified by copper(II) hexafluorosilicate," *Periodica Polytechnica Chemical Engineering*,vol. 66, pp. 304 – 312, 2022.

[6] A. Karakoc, M. Bulota, M. Hummel, S. Sriubaitė, M. Hughes, H. Sixta, and J. Paltakari, "Effect of single-fiber properties and fiber volume fraction on the mechanical properties of Ioncell fiber composites," *Journal of Reinforced Plastics and Composites*, vol. 40, pp. 741–748, 2021.

[7] A. H. D. Abdullah, N. Karlina, W. Rahmatiya, S. Mudaim, Patimah, and A. R. Fajrin, "Physical and mechanical properties of five Indonesian bamboos," *IOP Conference Series: Earth and Environmental Science*, vol. 60, p. 012014, 2017.

[8] I. D. Mohammadi, A. M. Poursattar, F. Sadegh, M. E. Soltani, M. Safaeirad, and M. Frediani, "Synthesis and characterization of flame retardant unsaturated polyester-allyloxysilane resin for wood coatings," *Scientific Reports*, vol. 14, pp. 1–15. 2024.

[9] *Standard practice for preparation of metallographic specimens*, ASTM E3-01, ASTM International, 2017.

[10] S*tandard Test Methods for Flexural Properties of Unreinforced and Reinforced Plastics and Electrical Insulating Materials*, ASTM D790-17, ASTM International, 2017.

[11] Test Method for Determination of Charpy Impact Strength (Withdrawn 1998), ASTM D5942-96, ASTM International, 2017.

[12] Z. Khan, B. F. Yousif, and M. Islam, "Fracture behaviour of bamboo fiber reinforced epoxy composites," *Composites Part B: Engineering*, vol. 16, pp. 186 – 199, 2017.

[13] M. Oliveira, V. Neves, and M. D. Banea, "Mechanical and thermal characterization of bamboo and interlaminar hybrid bamboo/ synthetic fibre-reinforced epoxy composites," *Materials*, vol. 17, no. 8, p. 1777, 2024.

[14] D. Wang, T. Bai, W. Cheng, C. Xu, G. Wang, H. Cheng, and G. Han, "Surface modification of bamboo fibers to enhance the interfacial adhesion of epoxy resin-based composites prepared by resin transfer molding," *Polymers*, vol. 11, no. 12, p. 2107, 2019.

[15] K. Zhang, F. Wang, W. Liang, Z. Wang, A. Duan, and B. Yang, "Thermal and mechanical properties of bamboo fiber reinforced epoxy composites," *Polymers*, vol. 10, no, 6, p. 608, 2018.

[16] B. A. Mebratie, B. S. Ayele, and A. A. Meku, "Investigating the tensile and flexural strength of sunflower oil treated *Ethiopian Highland* bamboo fibre reinforced polyester composites," *Advances in Bamboo Science*, vol. 3, p. 100021, 2023.

[17] M. Jawaid, S. Krishnasamy, C. Muthukumar, H. Fouad, M. Hashem, A. S. Ismail, R. Khiari, and B. Singh, "Investigating the effect of *Varied Short* bamboo fiber content on the thermal, impact, and flexural properties of green epoxy composites," *Journal of Natural Fibers*, vol. 21, no. 1, p. 2296915, 2024.

[18] J. Shi, Y. Wu, M. Zhang, J. Zhang, W. Zhang, H. Chen, Y. Peng, S. Q. Shi, and C. Xia, "Bamboo fiber-reinforced epoxy composites fabricated by vacuum-assisted resin transfer molding (VARTM): Effect of molding sequence and fiber content," *Polymer Composites*, vol. 45, no. 1, pp. 256–266, 2024.

[19] R. Kumar, A. Ganguly, and R. Purohit, "Optimization of mechanical properties of bamboo fiber reinforced epoxy hybrid nano composites by response surface methodology," *International Journal on Interactive Design and Manufacturing*, vol. 18, pp. 6479–92, 2024.

[20] A. C. Manalo, E. Wani, N. A. Zukarnain, W. Karunasena,K. T. Lau, "Effects of alkali treatment and elevated temperature on the mechanical properties of bamboo fibre-polyester composites," *Composites Part B: Engineering,* vol. 80, pp. 73–83, 2015.

[21] W. Zhang, C. Wang, S. Gu, H. Yu, H. Cheng, and G. Wang, "Physical-mechanical properties of bamboo fiber composites using filament winding," *Polymers*, vol. 13, p. 2913, 2021.

[22] M. Elkolali, L. P. Nogueira, P. O. Rønning, and A. Alcocer, "Void content determination of carbon fiber reinforced polymers: A comparison between destructive and non-destructive methods," Polymers, vol. 14, p. 1212, 2022.

[23] J. Jang, M. Maydison, Y. Kim, Z. Han, and D. Oh, "Effect of void content on the mechanical properties of GFRP for ship design," *Journal of Marine Science and Engineering*, vol. 11, p. 1251, 2023.

[24] P. Pączkowski, A. Puszka, and B. Gawdzik, "Investigation of degradation of composites based on unsaturated polyester resin and vinyl ester resin, *Materials*, vol. 15, p. 1286, 2022.

[25] J. Y. Chane-Ching, A. Lebugle, I. Rousselot, A. Pourpoint, and F. Pellé, "Colloidal synthesis and characterization of mono-crystalline apatite nanophosphors," *Journal of Materials Chemistry*, vol. 17, no. 28, pp. 2904–2913, 2007.

[26] O. Ozukanar, G. Sagdic, E. Çakmakçı, F. K. Özmen, M. E. Üreyen, U. S. Gunay, H. Dyrnazm, and V Kumbaraci, "Triazole-, piperazine, and DOPO -containing eugenol-based reactive flame retardant for unsaturated polyester resin," *Journal of Applied Polymer Science*, vol. 141, no. 43, p. e56127, 2024.

[27] B. Schartel, "Phosphorus-based flame retardancy mechanisms—old hat or a starting point for future development?," *Materials*, vol. 3, no. 10, pp. 4710–4745, 2010.

[28] S. M. Seraji, P. Song, R. J. Varley, S. Bourbigot, D. Voice, and H. Wang, "Fire-retardant unsaturated polyester thermosets: The state-of-the-art, challenges and opportunities," *Chemical Engineering Journal*, vol. 430, p. 132785, 2022.